

Non-linear Dynamics of the Kink Instability in Spheromak Configurations with Open Flux

Pablo L. García Martínez and Ricardo Farengo

Centro Atómico Bariloche and Instituto Balseiro, Bariloche, RN, Argentina

The relaxation of decaying, kink unstable, spheromak equilibria with open flux is investigated using 3D resistive MHD simulations. The force free equilibria are characterized by a stepwise current profile, which includes a high parallel current on the open flux region. When the open flux current is high enough, the configuration becomes kink unstable. The nonlinear evolution of several kink unstable equilibria is analyzed.

Simulation Description

Using the VAC code [1], we solve the 3D, isothermal resistive MHD equations employing a TVD finite volume method with a Roe-type Riemann solver. The $\nabla \cdot \mathbf{B} = 0$ condition is maintained using the projection method. To simplify the physics, we do not advance the density. This corresponds to a constant pressure computation, usually referred to as the zero- β approximation, widely used when modeling low- β plasmas. A uniform cartesian grid is used to advance the equations in time and a poloidal grid containing the Fourier coefficients of the toroidal decomposition is employed to analyze the results.

The geometry employed corresponds to a gun produced spheromak with a cylindrical flux conserver and electrodes at one end. The elongation is 1 and the boundary conditions imposed (interpolating from the cartesian grid) at the flux conserver are $\mathbf{B} \cdot \mathbf{n} = 0$ and $\mathbf{J} \times \mathbf{n} = 0$. At the electrode end ($z=0$) the poloidal flux is prescribed (see below).

The initial conditions employed in the simulations are force-free equilibria obtained by solving the Grad-Shafranov equation with λ ($\lambda = \mu_0 \mathbf{J} \cdot \mathbf{B} / B^2$) taken as a function of the poloidal flux:

$$\lambda(\psi) = \lambda_c + \frac{\lambda_c - \lambda_a}{2} \{ \tanh[\delta(1 - \psi)] - 1 \}$$

The boundary condition employed to calculate the equilibria are $\psi = 0$ at the flux conserver walls and $\psi(r, z=0) = C r^2 (1-r)^3$ at the electrode end (see Ref. [2] for details).

The MHD equations are normalized using a length scale R (the flux conserver radius), a density scale ρ_0 and a typical magnetic field B_0 . With these quantities we define the Alfvén ($\tau_A=R\sqrt{\rho_0/B_0}$) and resistive ($\tau_r=1/\eta\lambda_{\text{Taylor}}^2$) times and the Lundquist number ($S=\tau_A/\tau_r$), where η is the resistivity and λ_{Taylor} is the first eigenvalue corresponding to the Taylor state (uniform λ). In what follows, the time is indicated in units of τ_A , the lengths in units of R and $S\approx 2000$.

Results

In Fig. 1, left side, we show the evolution of the total magnetic energy and the energy in the $n=0$ mode (a), the energy content of the $n=1, 2$ and 3 modes (b), the poloidal and toroidal fluxes (c) and the ratio between the magnetic energy and the relative helicity (defined to be gauge invariant) (d). It is clear that the growth and non linear interaction of the unstable modes triggers a relaxation event that begins around $t\approx 100$ and lasts until $t\approx 170$. This event is characterized by a sharp drop in the ratio between the energy and the helicity, an increase in the poloidal flux and a reduction in the toroidal flux.

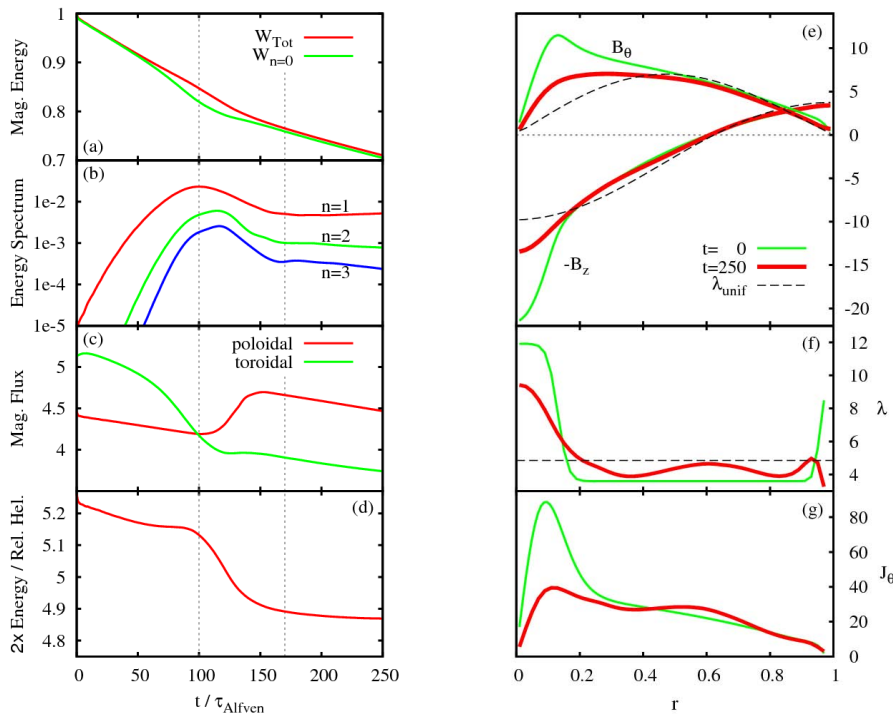


Fig. 1, time evolution of different quantities (a-d) and initial and final radial profiles of the magnetic field (e), λ (f) and the toroidal current density (g).

In the right side of Fig 1 we show the initial and final radial profiles, at $z=0.5$, of the magnetic field (e), λ (f) and the toroidal current density (g). The dashed line in Fig. 2f indicates the value corresponding to the uniform λ case that has the same relative helicity that the solution at $t=250$ (with the same boundary condition).

The fluctuations destroy the closed flux surfaces thus reducing plasma confinement. This is clearly shown in the puncture plots presented in Fig. 2 (upper left). In these plots, the blue lines begin at the electrodes while the red ones begin at the inner region. Only at $t=170$, when the amplitude of the unstable modes has decreased considerably, closed flux surfaces reappear. Fig. 2 also shows (bottom left) color maps of the parallel component of the dynamo electric field, which is defined as: $E_{d//} = \langle \mathbf{u} \times \mathbf{b} \rangle \cdot \mathbf{B}_{n=0} / B_{n=0}$, where \mathbf{u} and \mathbf{b} are the fluctuating parts of the velocity and magnetic field and $\langle \cdot \rangle$ indicates the toroidal average. The black contour indicates the $E_{d//} = 0$ boundary. At $t=100$ a strong antidynamo localizes near the symmetry axis while a relatively weak dynamo appears in the central region. At $t=140$ there is a strong dynamo at the magnetic axis and a weak dynamo in the rest of the plasma. Finally, at $t=170$ a complex structure appears with weak dynamos and antidynamos in different regions. This is probably responsible for the final flattening of the λ profile.

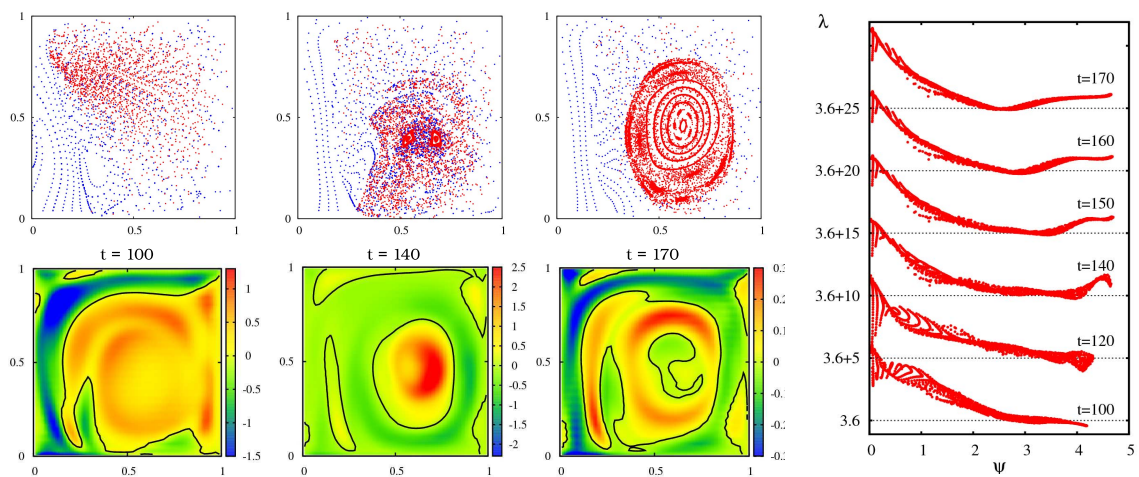


Fig. 2. Left: puncture plots and contours of constant dynamo field at different times. Right: λ profiles at different times.

The right side of Fig. 2 shows λ as a function of the poloidal flux at several times during the relaxation period (different times are separated from each other by a vertical offset of 5 units). In a perfectly axisymmetric equilibrium there should be only one value of λ for each value of ψ . However, when the axisymmetry is destroyed by the fluctuations this is no longer true. In agreement with the puncture plots, it is seen that at $t=170$ the plot begins to collapse into a single line. On the other hand, it is observed that the evolution of the dynamo produces a wave like motion in the $\lambda(\psi)$ profile.

In Fig. 3a we show the flux amplification factor, A , defined as the ratio between the poloidal flux at the magnetic axis Ψ_{ma} and the gun flux Ψ_G , as a function of time for $\lambda_c = 12$ and three values of λ_a . The three cases are kink unstable but the behavior of A changes significantly with relatively small changes in λ_a . When $\lambda_a = 3.8$ the flux generated by the fluctuations is not enough to prevent A from decreasing rapidly. When $\lambda_a = 3.4$ (most unstable case) a large flux amplification occurs and the final A is larger than the initial one. Finally, when $\lambda_a = 3.6$, A oscillates around 4.4 and we can conclude that the relaxation process produces just enough flux to sustain the configuration. In Fig. 3b we show the ratio between the magnetic energies of the $n=1$ and $n=0$ modes. This is an important parameter because it indicates the level of fluctuations that would be needed to sustain the configuration. Fig. 3c shows A for four different pairs of values of λ_a and λ_c . It is clear that, for each value of λ_c , it is possible to trigger relaxation processes that keep A approximately constant by selecting appropriate values of λ_a . The level of fluctuations resulting in these cases is shown in Fig. 3d. It is interesting to note that the smallest values of A require the largest relative values of the fluctuations and vice versa.

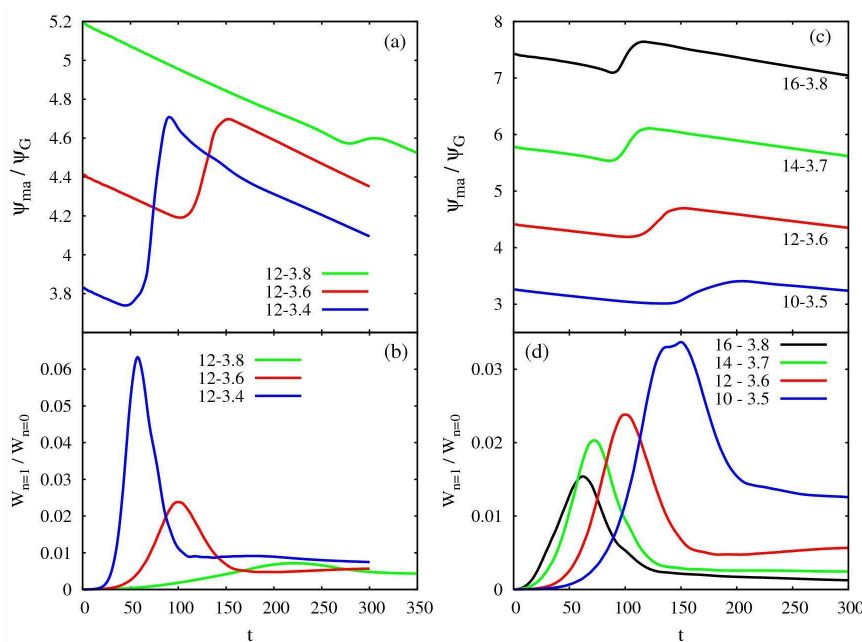


Fig. 3. Flux amplification and ratio of magnetic energy between the $n=1$ and $n=0$ modes.

[1] G Toth, VAC code (www.phys.uu.nl/~toth/)

[2] D P Brennan *et al* 2002 Phys. Plasmas **9** 3526.